α-particle production in ^{6}He + ^{120}Sn collisions

P. N. de Faria,[1] R. Lichtenthäler,[1] K. C. C. Pires,[1] A. M. Moro,[2] A. Lépine-Szily,[1] V. Guimarães,[1]
D. R. Mendes Jr.,[1] A. Arazi,[3] A. Barioni,[1] V. Morcelle,[1] and M. C. Morais[1]
[1]*Instituto de Fisica, Universidade de São Paulo, Caixa Postal 66318, 05314-970 São Paulo, Brazil*
[2]*Departamento de FAMN, Universidad de Sevilla, Apartado 1065, E-41080, Sevilla, Spain*
[3]*Laboratorio Tandar, Departamento de Fisica, Comisión Nacional de Energía Atómica,*
Avenida del Libertador 8250 (1429), Buenos Aires, Argentina
(Received 17 May 2010; published 9 September 2010)

The collision ^{6}He + ^{120}Sn has been investigated at four energies near the Coulomb barrier. A large yield of α particles has been detected, with energies around the energy of the scattered ^{6}He beam. The energy and angular distributions of the α particles have been analyzed and compared with breakup and neutron transfer calculations.

DOI: 10.1103/PhysRevC.82.034602 PACS number(s): 21.45.−v, 24.10.Ht, 24.10.Eq, 25.60.−t

I. INTRODUCTION

The elastic scattering and reactions induced by low-energy neutron-rich and proton-rich projectiles on heavy and medium-mass targets have been studied over recent years. A large total reaction cross section has been reported [1–4], compared to stable systems of the same mass. The reaction channels responsible for this large total cross section have not yet been completely identified although the projectile breakup, fusion, and one- and two-neutron stripping reactions are considered to be most important candidates. An intriguing question is how to separate the contributions from reactions proceeding via the equilibrated compound system (fusion) from other direct reaction channels. In fact, in the case of reactions induced by light exotic projectiles, one expects a mixing of the two scenarios. Because of the low binding energies and spatially extended distributions of nucleons in the projectile, there is a large probability that some nucleons of the projectile will fuse with the target, leaving a highly excited recoil nucleus, while the remaining projectile fragment follows with an energy and angular distribution typical of a direct reaction. This is the so-called incomplete fusion process. On the other hand, Q-optimum considerations indicate that the direct transfer of nucleons to excited states of the target below the particle emission thresholds (bound states) is very likely to occur. In principle, coincidence measurements between charged particles, neutrons, and γ rays emitted during the reaction should provide us with means to reconstruct the kinematics of the reaction and distinguish between different mechanisms. However, with the present intensities and quality of the secondary beams, strong restrictions are imposed on the experiments. Despite these difficulties, experiments have been performed, using neutron–α-particle coincidence techniques [5–7], which allow the identification of the breakup and 1n- and 2n-transfer reaction channels in the ^{6}He + ^{209}Bi scattering. More recently, the detection of the α-particle fragments in triple coincidence with neutrons and γ rays of the decay of the residual nucleus in the collision of ^{6}He + ^{65}Cu [8] allowed the identification of the 1n and 2n neutron transfers as important reaction channels. Despite the difficulties of the coincidence measurements, the analysis of the energy distribution of the charged particles emitted in the reactions can, in some cases, give some valuable information about the reaction mechanism.

In this article we present an analysis of the energy and angular distributions of the α particles emitted in the ^{6}He + ^{120}Sn collision at four energies 17.4, 18.05, 19.8, and 20.5 MeV. We compare the experimental results with the theoretical predictions for several processes, namely, projectile breakup, 1n and 2n transfer, and fusion-evaporation.

II. EXPERIMENTAL MEASUREMENTS AND RESULTS

The experiment was performed in the 8UD São Paulo Pelletron Laboratory using the Radioactive Ion Beams in Brasil (RIBRAS) system [9,10]. The ^{7}Li primary beam of energies in the range $E_{\rm lab}$ = 24–26 MeV and intensities of about 300 nA e was focused on a 12 μm ^{9}Be foil in which the ^{6}He beam was produced via the ^{9}Be(^{7}Li,^{6}He)^{10}B reaction. The ^{6}He beam was collected and focused by the first solenoid on the secondary target position. A more detailed explanation of the RIBRAS system can be found in [1]. A 3.8 mg/cm^{2} ^{120}Sn (98.29%) foil was used as secondary target. An array consisting of four ΔE(20 μm)-E(1000 μm) silicon telescopes allows the detection and identification of the charged particles emerging from the reaction. In Fig. 1 we present some ΔE-$E_{\rm total}$ spectra, where $E_{\rm total} = E + \Delta E$. We clearly see the ^{6}He particles elastically scattered in the target as well the ^{7}Li^{2+} beam contaminants. In the biparametric spectrum of Fig. 1 one observes a group of counts along the α-particle line, at energies near to the energy of the ^{6}He elastic peak. The α-particle energies are distributed over a broad region centered around 2/3 of the energy of the scattered ^{6}He. In Fig. 2 (left) we present the α-particle energy spectra projected on the total energy axis. The energy axis was obtained from the total energy signal ($E_{\rm total}$) by summing up the energy losses of the α particles in one-half of the target thickness, assuming that the reaction took place in the middle of the target. Because of the low statistics we summed the spectra at a few angles around 50°–75° where the peak is more visible and calculated the double differential cross sections $d^{2}\sigma/d\Omega dE$. The energies plotted in the x axis and the cross sections can be directly compared to theoretical calculations. In Fig. 2 (right) we present also the angular distributions of the α group. The angular distributions were obtained by integrating the counts of the entire α group in an energy region of about ±4 MeV

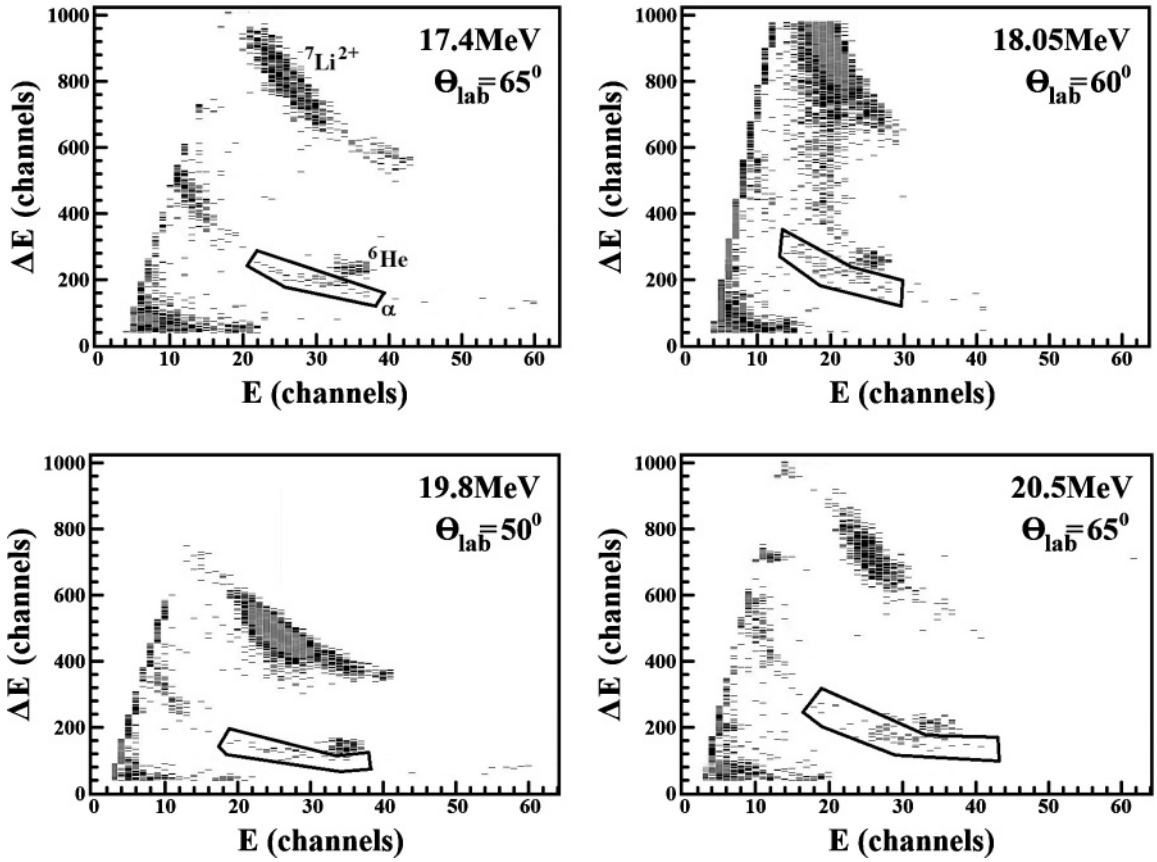

FIG. 1. ^{6}He + ^{120}Sn biparameteric spectra. The α-particle group is shown inside the poligon and the peak above corresponds to the ^{6}He + ^{120}Sn elastic scattering

around the centroid of the distribution. The normalization of the absolute cross sections was obtained using the gold target runs as described in [1].

III. ANALYSIS OF THE α-PARTICLE PRODUCTION CHANNEL

The energies of the particles produced in a reaction depend on the kinematics of the reaction and the excitation energies of the nuclei populated in the exit channel. In order to disentangle the reaction mechanisms responsible for the production of these α particles, the measured distributions have been compared with theoretical calculations assuming three possible reaction mechanisms, namely, elastic breakup to the ^{6}He continuum, 1n and 2n transfers from the projectile to the target, and particle evaporation following the formation of a compound nucleus. The results of the calculations are displayed in Fig. 2 and will be discussed in the next subsections.

A. The projectile direct breakup

Within a direct breakup picture, the 2n removal channel is interpreted as an inelastic excitation of the ^{6}He projectile to its continuum states. The relevance of this mechanism has been investigated by means of continuum-discretized coupled-channels (CDCC) calculations. One has to bear in mind, however, that the breakup cross sections provided by this method are referred to the $\alpha + n + n$ center of mass. In principle, the α cross sections can be obtained from the CDCC breakup amplitudes by applying the appropriate kinematic transformation. This transformation has been already developed and applied to three-body CDCC (3b-CDCC) calculations [11], namely, a two-body projectile scattered by a target. An accurate treatment of the ^{6}He + ^{120}Sn reaction would require a four-body reaction model. Although four-body CDCC calculations (4b-CDCC) are currently available for ^{6}He reactions [12], convergence of the breakup observables has not yet been fully achieved and, in addition, the transformation to obtain the α-particle observables is still to be developed. For these reasons, we rely here on the 3b-CDCC calculations presented in Ref. [1]. Given the reasonable agreement found in that work for the elastic scattering between the 3b-CDCC and 4b-CDCC calculations, we believe that the breakup cross sections extracted from the former can provide us with a realistic estimate of this observable. In these 3b-CDCC calculations, we use the dineutron model proposed in Ref. [13]. In this model, the two halo neutrons are treated as a structureless cluster coupled to spin zero, bound to the α core with an effective separation energy of 1.6 MeV. Continuum states are also treated within an $\alpha + 2n$ model. Further details of the model and the CDCC calculations can be found in Refs. [13] and [1], respectively. For the calculation of the α cross sections

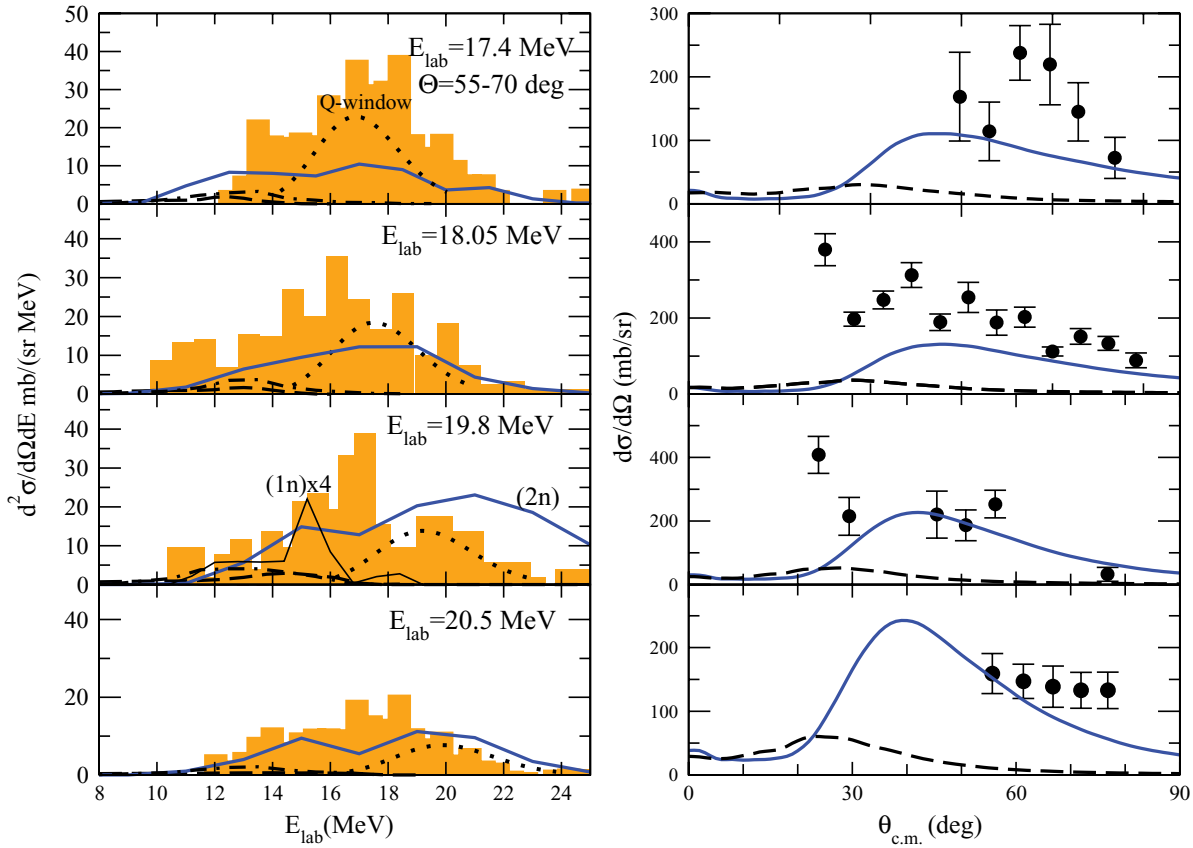

FIG. 2. (Color online) Energy spectra (left) and the corresponding angular distributions (right) of the α particles produced in the reaction ^{6}He + ^{120}Sn. The histogram (left) and the filled circles (right) are the experimental data. The dotted Gaussian stands for the Q window for the $2n$ transfer process, arbitrarily normalized. The solid line corresponds to the two-neutron distorted-wave Born approximation (DWBA) transfer calculation without any normalization. The dashed line corresponds to the breakup calculation without any normalization and the dot-dashed stands for the fusion-evaporation Projection Angular-momentum Coupled Evaporation (PACE) calculation arbitrarily normalized. The thin solid line plotted at $E = 19.8$ MeV (left) is the $1n$ DWBA calculation, multiplied by a factor of 4 to make the curve more visible.

from the breakup scattering amplitudes, we used the formalism and the codes developed in the work of Tostevin *et al.* [11].

The calculated energy distributions are shown in Fig. 2 (left) by dashed lines. It is seen that the calculations underpredict the observed α-particle energies. In addition, the measured α yield can not be accounted for by the 3b-CDCC calculations. This is shown in Fig. 2 (right), where we see that these calculations cannot reproduce either the shape or the magnitude of the measured angular cross section. The observed α yields are underestimated by about one order of magnitude, depending on the energy. The shape of the 3b-CDCC angular distributions indicates that the direct breakup mechanism should become more important at forward angles rather than at backward angles, where most of the α particles are observed. We then conclude that the direct breakup mechanism can be responsible for some of the observed α particles, but it is certainly not the main process involved.

B. The neutron transfer reactions

The measured α particles can also be interpreted as coming from the one-neutron ^{120}Sn(^{6}He,^{5}He)^{121}Sn or two-neutron ^{120}Sn(^{6}He,α)^{122}Sn stripping reactions. The ^{5}He nucleus is unbound and decays into one neutron plus an α particle. It is well known that particle transfer reactions have large cross section only for a window of $Q_{\rm reac}$ values centered at the optimum Q value which can be estimated by the simple expression [14,15]:

$$Q_{\rm opt} = E_{\rm c.m.}\left(\frac{Z_{pf}Z_{tf}}{Z_{pi}Z_{ti}} - 1\right), \qquad (1)$$

where $Z_{p,t,i,f}$ stand for the atomic numbers of the projectile and target in the initial and final channels. Since the reaction Q value is obtained as the difference between the binding energies of the transferred particle in the final and the initial channels, $Q_{\rm reac} = E_{Bf} - E_{Bi}$ with $E_B > 0$ for bound states and $E_{Bf} = E_{Bf}^{gs} + E_x$, the condition $Q_{\rm opt} = Q_{\rm reac}$ basically defines a region of excitation energies E_x in the final nucleus that will be populated. For the case of neutron transfer $Q_{\rm opt} = 0$ and $E_{Bf} \approx E_{Bi}$. For weakly bound projectiles, the initial binding energy E_{Bi} is small and, as a consequence, E_{Bf} will also be small, thus resulting in the population of highly excited states in the final nucleus. Figure 3 shows an excitation energy scheme which illustrates this idea for the $2n$ transfer reaction ^{120}Sn(^{6}He,α)^{122}Sn. It is seen that the $2n$ transfer populates states between the $1n$ and $2n$ thresholds.

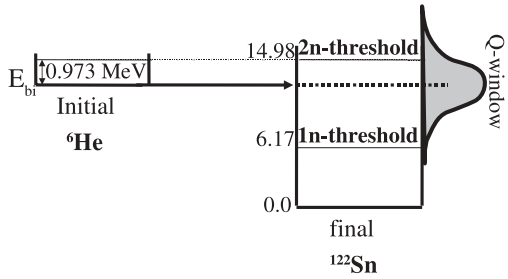

FIG. 3. Scheme showing the excitation energy region populated by the $2n$ transfer leading to the ^{122}Sn nucleus. The separation energies S_{1n} and S_{2n} for the ^{122}Sn nucleus are indicated in MeV.

1. *Two-neutron transfer*

The dotted line in Fig. 2 (left) is the result of a Q-window calculation (arbitrarily normalized) using a Gaussian shape (Ref. [15]) centered at the $Q_{\rm opt}$ [see Eq. (1)] and considering the kinematics of the $2n$ transfer reaction ^{120}Sn(^{6}He,α)^{122}Sn. This simple Q-optimum calculation shows that the $2n$ transfer would produce α particles within the energy range of the measurements.

To evaluate the importance of this mechanism we have performed DWBA calculations for the two-neutron transfer process, including states below and above the $2n$ threshold. These calculations have been performed using the transfer to the continuum (TC) method [16,17], using the FRESCO code [18]. The distorted waves of the incoming channel were generated with the optical potentials derived in Ref. [1] from the fit of the elastic data. For the core-core interaction (^{4}He + ^{120}Sn), as well as for the exit channel optical potential, we used the α interaction of Ref. [19]. The internal wave function of the ^{6}He nucleus is calculated assuming the same dineutron model used in the 3b-CDCC calculations. The dineutron cluster is assumed to be transferred as a single entity to ^{122}Sn states. For the orbital angular momentum associated with the $2n$-^{120}Sn motion, l_f, we considered values from $l_f = 0$ to $l_f = 8$. For each value of l_f, the continuum was discretized using bins of 1 MeV width, up to a maximum excitation energy of 9 MeV above the $2n$ breakup threshold. For the states below this threshold, we considered a set of representative states, distributed at intervals of 1 MeV, following the same procedure proposed in Ref. [16]. For each l_f, the number of nodes of the $2n$-^{120}Sn motion was determined from the Wildermuth condition (see, e.g., Ref. [20]), assuming that the transferred neutrons populate the lowest unoccupied single-particle states according to a simple shell-model picture to produce the state with the desired total angular momentum. For the transfer couplings, the post form of the transition operator was used.

The calculated cross sections were transformed to the laboratory frame with the appropriate Jacobian. The resulting angular and energy distributions are compared with the data in Fig. 2 without any normalization (solid lines). The shape of the angular distributions is in reasonable agreement with the data, indicating that the two-neutron transfer mechanism can play an important role. The angle-integrated $2n$ cross section is $\sigma_\alpha \approx 650$ mb. This value remains approximately constant for the four energies and is of the order of $\sigma_{\rm halo}$ [1] obtained from the elastic scattering analysis. It is clear from Fig. 2 that the TC calculation underestimates a little the experimental cross sections. In this case, the angle-integrated cross section for the α particles would be even larger than 650 mb. Given that the total reaction cross section is determined independently from the elastic scattering [1], a larger total α cross section would imply a smaller complete fusion cross section. Here we assume that the α cross section is coming entirely from a direct process and the complete fusion does not contribute to the α peak. This will be discussed in more detail in Sec. III C. A possible suppression of the fusion cross section is an expected result for neutron-rich exotic systems above the barrier; however, given the uncertainties in the determination of the total cross sections, a definite conclusion about this issue is not possible.

One has to bear in mind also that part of the discrepancies between the calculations and the data can arise from the approximations involved in these calculations. In particular, we use a very simple model for both the reaction mechanism and the structure of the initial and final nuclei. A proper treatment of this process would require a three-body description of the ^{6}He nucleus as well as a more realistic description of the ^{122}Sn two-neutron states. In addition, the calculations do not include any information on the $2n$ spectroscopic factor for the final nucleus, which, within the DWBA approximation, would affect the absolute normalization of the calculations. Notwithstanding these limitations, we believe that our schematic calculations are sufficiently realistic to support the conclusion that the $2n$ transfer mechanism is a very important mechanism in this reaction at the measured angles. These conclusions are in agreement with those found in other ^{6}He-induced reactions [16,21,22].

Despite the large differences found between the direct breakup (CDCC) and TC calculations, it is worth noticing that, strictly speaking, the states included in these TC calculations are not completely orthogonal to those included in the direct breakup calculations, and therefore their respective contributions cannot be simply added. In this sense, the direct breakup and transfer calculations should be considered as two different reaction models, each of them emphasizing a different set of final states; final states with low relative energy and angular momentum between the neutrons and the α core are expected to be better described within the direct breakup model, whereas the transfer to the continuum method will be more suited to describe final states with small energy and angular momentum with respect to the target. In practice, because of the model space truncation required in both calculations and the different choice of the interactions, we do not expect the two calculations to provide the same results [17]. Furthermore, the fragment-target interactions that enter the CDCC calculations use optical potentials that describe the corresponding elastic scattering and, therefore, only the elastic breakup component is accounted for by this method.

2. *One-neutron transfer*

We have considered also the reaction ^{120}Sn(^{6}He,^{5}He)^{121}Sn and the subsequent breakup of the ^{5}He $\rightarrow \alpha + n$. We

performed DWBA calculations using the code FRESCO [18]. Because of the large number of excited levels in the ^{121}Sn nucleus and the considerable spreading of the single-particle strength at the excitation energies around the optimum Q value, we did not attempt to include the physical states in this calculation. Instead, we assumed a simple model in which, for each single-particle configuration, the single-particle strength is distributed among a set of representative states of ^{121}Sn that cover the region of excitation energies around the optimum Q value. In particular, the following single-particle levels were included: $2d_{3/2}$, $1h_{11/2}$, $3s_{1/2}$, $1g_{7/2}$, $2d_{5/2}$, $2f_{7/2}$, and $3p_{3/2}$. For each configuration, we considered a set of five states at the excitation energies 0.919, 1.919, 2.919, 3.919, and 4.919 MeV. These energies were chosen to cover the region from the low-lying states up to the one-neutron breakup threshold (6.171 MeV) of ^{121}Sn in steps of 1 MeV. Three additional bins at 1.5, 2.5, and 3.5 MeV excitation energies above the $1n$ threshold were considered for each configuration. The spectroscopic factor for each representative state was taken as the sum of the experimental levels located around the excitation energies considered (see Table I in Ref. [23]). For the unbound states we used $S = 1$. For the projectile overlap $\langle^{5}\mathrm{He}|^{6}\mathrm{He}\rangle$, we assumed a $p_{3/2}$ configuration with spectroscopic factor $S = 2$. The bound state wave functions for the final states were calculated using a Woods-Saxon well potential, with reduced radius $r_0 = 1.25$ fm and diffuseness $a = 0.65$ fm, and the depth adjusted to reproduce the appropriate one-neutron separation energy. The real part of the incoming optical potential was generated using the São Paulo double-folding potential. The imaginary part was parametrized in terms of a Woods-Saxon shape with parameters $V_0 = 28.8$ MeV, $R_i = 1.34 \times 120^{1/3}$ fm, and $a_i = 1.185$ fm. The core-core interaction ($^{5}\mathrm{He} + ^{120}\mathrm{Sn}$), which appears in the remnant part of the transition operator, as well as the exit channel optical potential ($^{5}\mathrm{He} + ^{121}\mathrm{Sn}$), were also represented by the same potential used for the incoming channel. The post form of the transition amplitude was used. The calculated cross sections were converted to the laboratory frame by applying the appropriate kinematic transformation, and the energy of the α particles was calculated as $E_\alpha = 0.8E_{^{5}\mathrm{He}}$. Here we make the simplifying assumption for the breakup process that the outgoing α particle takes a fraction $m_\alpha/m_{^{5}\mathrm{He}}$ of the ^{5}He kinetic energy. This can be justified by the fact that, in the ^{5}He frame, the neutron takes most of the breakup energy ($E_{\mathrm{bup}} = 890$ keV, $E_n = 712$ keV); however, the remaining α-particle energy ($E_\alpha = 178$ keV) might produce a non-negligible broadening of a few MeV on the energy of the α particles. The result is shown by the thin solid line in Fig. 2 (left) for the incident energy of 19.8 MeV. Although the calculated $1n$ yield has been multiplied by a factor of 4 (see Fig. 2), we see that the one-neutron transfer could contribute to the low-energy region.

C. Fusion

Part of the observed α yield might arise from evaporation following the formation of a compound nucleus. To evaluate the importance of this channel, we have performed complete fusion and decay calculations using the PACE program [24]. The complete fusion calculations for ^{6}He + ^{120}Sn show that the compound nucleus ^{126}Te would decay mainly by emitting neutrons and only a small fraction of the cross section (a few milibarns) would decay through α-particle emission. Cross sections of this order would not be detectable in our experiment. The calculated energy distribution of the evaporated α particles is shown in Fig. 2 (left) at 19.8 MeV and is centered in the low-energy tail of the data in the same region populated by the breakup. However, because of the low cross section, we do not expect that the α particles coming from the complete fusion would be seen in this experiment. We considered also the incomplete fusion of an α particle with 2/3 of the laboratory energy of the ^{6}He forming the ^{124}Te compound nucleus and the decay by α particles is still less probable than in the case of complete fusion. Thus we do not believe that complete fusion would give any significant contribution to the observed α yield.

IV. CONCLUSIONS

A large yield of α particles has been observed in the ^{6}He + ^{120}Sn reaction measured at energies around the Coulomb barrier. The angular and energy distributions of these α particles have been compared with several reaction models, in order to disentangle the dominant reaction mechanisms. A kinematic analysis of the energy distributions leads to the conclusion that the neutron stripping transfer reactions are probably the dominant mechanisms contributing to the observed α yield. DWBA calculations and simple Q-optimum considerations indicate that the α particles are probably produced in $2n$- and $1n$-stripping reactions to excited states of the final nucleus (^{122}Sn and ^{121}Sn, respectively). CDCC calculations show that the projectile breakup mechanism contributes only to the lower-energy region of the observed α spectrum. However, the magnitude of the calculated cross sections are found to be of the order of a few tens of millibarns, whereas the experimental cross section is on the order of a few hundreds of millibarns. This indicates that the direct breakup mechanism alone cannot explain the observed yields. Two-neutron transfer calculations, performed within the DWBA approximation, gave cross sections which agree better with the experimental results. The $2n$-transfer angle-integrated cross sections are compatible with the total reaction cross sections measured from the elastic angular distributions.

ACKNOWLEDGMENTS

The authors thank the Fundação de Amparo à Pesquisa do Estado de São Paulo (FAPESP) and the Conselho Nacional de Desenvolvimento Científico e Tecnológico (CNPq) for financial support. This work has been partially supported by the Complementary Action PCI2006-A7-0654, funded by the Spanish Ministry of Education and Science. A.M.M. acknowledges the support by Spanish Ministerio de Ciencia e Innovación under Project No. FPA2006-13807-c02-01, the local government of Junta de Andalucía under the Excellence Project No. P07-FQM-02894, and the Spanish Consolider-Ingenio 2010 Programme CPAN (CSD2007-00042).

[1] P. N. de Faria *et al.*, Phys. Rev. C **81**, 044605 (2010).
[2] N. Keeley, J. M. Cook, K. W. Kemper, B. T. Roeder, W. D. Weintraub, F. Marechal, and K. Rusek, Phys. Rev. C **68**, 054601 (2003).
[3] E. F. Aguilera *et al.*, Phys. Rev. C **79**, 021601(R) (2009).
[4] J. M. B. Shorto *et al.*, Phys. Lett. B **678**, 77 (2009).
[5] J. P. Bychowski *et al.*, Phys. Lett. B **596**, 26 (2004).
[6] J. J. Kolata *et al.*, Phys. Rev. C **75**, 031302(R) (2007).
[7] P. A. DeYoung *et al.*, Phys. Rev. C **71**, 051601(R) (2005).
[8] A. Chatterjee *et al.*, Phys. Rev. Lett. **101**, 032701 (2008).
[9] R. Lichtenthäler *et al.*, Eur. Phys. J. A **25**, s01, 733 (2005); Nucl. Phys. News **15**, 25 (2005).
[10] E. A. Benjamim *et al.*, Phys. Lett. B **647**, 30 (2007).
[11] J. A. Tostevin, F. M. Nunes, and I. J. Thompson, Phys. Rev. C **63**, 024617 (2001).
[12] M. Rodríguez-Gallardo, J. M. Arias, J. Gomez-Camacho, A. M. Moro, I. J. Thompson, and J. A. Tostevin, Phys. Rev. C **80**, 051601 (2009); M. Rodríguez-Gallardo, J. M. Arias, J. Gomez-Camacho, R. C. Johnson, A. M. Moro, I. J. Thompson, and J. A. Tostevin, *ibid.* **77**, 064609 (2008); T. Matsumoto, T. Egami, K. Ogata, Y. Iseri, M. Kamimura, and M. Yahiro, *ibid.* **73**, 051602 (2006); T. Matsumoto *et al.*, Nucl. Phys. A **738**, 471 (2004).
[13] A. M. Moro, K. Rusek, J. M. Arias, J. Gomez-Camacho, and M. Rodriguez-Gallardo, Phys. Rev. C **75**, 064607 (2007).
[14] D. M. Brink, Phys. Lett. B **40**, 37 (1972).
[15] R. A. Broglia and A. Winther, Phys. Rep. **4**, 153 (1972), (see pg. 191).
[16] D. Escrig *et al.*, Nucl. Phys. A **792**, 2 (2007).
[17] A. M. Moro and F. M. Nunes, Nucl. Phys. A **767**, 138 (2006); A. M. Moro *et al.*, *ibid.* **787**, 463c (2007).
[18] I. J. Thompson, Comput. Phys. Rep. **7**, 167 (1988).
[19] S. L. Tabor, B. A. Watson, and S. S. Hanna, Phys. Rev. C **11**, 198 (1975).
[20] G. R. Satchler, *Direct Nuclear Reactions* (Oxford University Press, New York, 1983), p. 721.
[21] R. Raabe *et al.*, Nature (London) **431**, 823 (2004).
[22] E. F. Aguilera *et al.*, Phys. Rev. Lett. **84**, 5058 (2000); Phys. Rev. C **63**, 061603(R) (2001).
[23] M. J. Bechara and O. Dietzsch, Phys. Rev. C **12**, 90 (1975).
[24] A. Gavron, Phys. Rev. C **21**, 230 (1980).